Abdom Imaging 28:416–432 (2003)
DOI: 10.1007/s00261-002-0052-0

Abdominal Imaging

Pictorial essay

CT of the acute abdomen: gynecologic etiologies

G. L. Bennett, W. B. Harvey, C. M. Slywotzky, B. A. Birnbaum
Department of Radiology, New York University Medical Center, Tisch Hospital, Room HW202, 560 First Avenue, New York, NY 10016, USA

Ultrasound has traditionally served as the first-line imaging procedure of choice for evaluation of the female patient with suspected pelvic or gynecologic pathology. However, the etiology of patient symptoms often is not certain at the time of presentation. As the role of computed tomography (CT) in the evaluation of patients with acute abdominal pain continues to rapidly expand, CT may be performed as the initial diagnostic imaging procedure. Further, in the setting of primary gynecologic pathology, CT offers more comprehensive evaluation than ultrasound because of the larger scan field of view. It is, therefore, important to be able to recognize the CT features of acute gynecologic disorders and differentiate them from disorders of the gastrointestinal or genitourinary tract. With the advent of multidetector CT scanning, improved multiplanar reformatted images may serve as a useful adjunct to cross-sectional imaging.

In this review, we present the CT findings in acute disorders of the female pelvis, including disorders of the adnexa, uterus, and postoperative/postpartum complications. We provide ultrasound correlation to show the complementary roles of these modalities in the evaluation of the female pelvis.

CT technique

Before performing CT in any young female patient, pregnancy must always be excluded. Optimized CT evaluation of suspected pelvic pathology requires administration of oral and intravenous contrast media. Opacification of the gastrointestinal tract with oral contrast (2% iodinated water-soluble contrast or 2.1%, w/v, barium sulfate suspension) allows for the distinction of bowel from adnexal structures. Intravenous contrast allows for better delineation of the uterus and adnexa. Although patterns of uterine enhancement vary with patient age and menstrual status, transitory zonal distribution of contrast in the myometrium and cervix may be appreciated with dynamic contrast-enhanced helical CT [1]. With the single-slice helical CT technique, images are obtained from the level of the iliac crests to the pubic symphysis with 5-mm collimation. These are reconstructed at 4 mm, with a pitch of 1.5. We administer 100–150 mL of 60% iodinated intravenous contrast at a rate of 1.5–2 mL/s, with a scan delay of 70–90 s. Delayed images are helpful for identification of the ureters. For multislice helical CT technique, we acquire images of the abdomen and pelvis by using a 4- $\times$ 2.5-mm detector configuration and a pitch of 6–7. With a rotation time of 0.5–0.8 s, this allows for 30 mm of coverage per second and a nominal slice thickness of 2.5 mm. This technique enables acquisition of improved multiplanar reformation.

The adnexa

Ovarian torsion

Ovarian torsion accounts for approximately 3% of all emergent gynecologic surgeries and results from adnexal rotation with twisting of the vascular pedicle and resultant venous, arterial, and lymphatic obstruction [2]. This may occur in the absence of ovarian pathology in children and adolescents. In adults, however, torsion usually is associated with an ovarian mass, most frequently the mature cystic teratoma [3], which serves as a fulcrum for torsion.

If ovarian torsion is the primary diagnostic consideration, Doppler ultrasound is the imaging study of choice. Diagnostic findings include an enlarged ovary with pe-

Correspondence to: G. L. Bennett

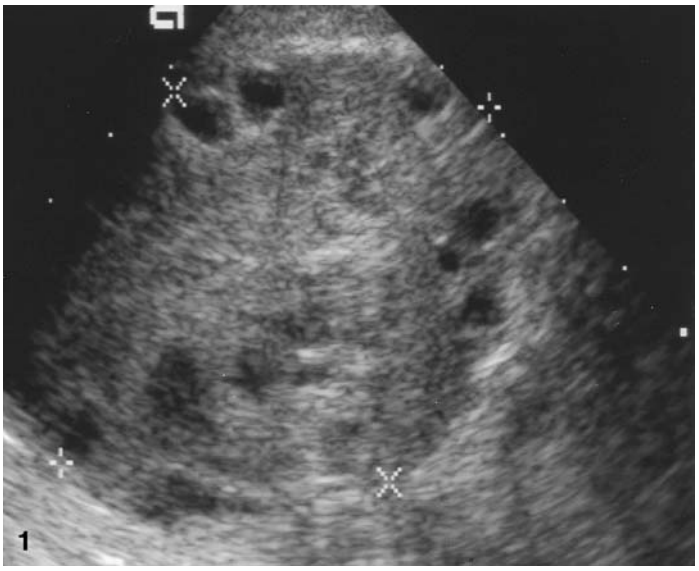

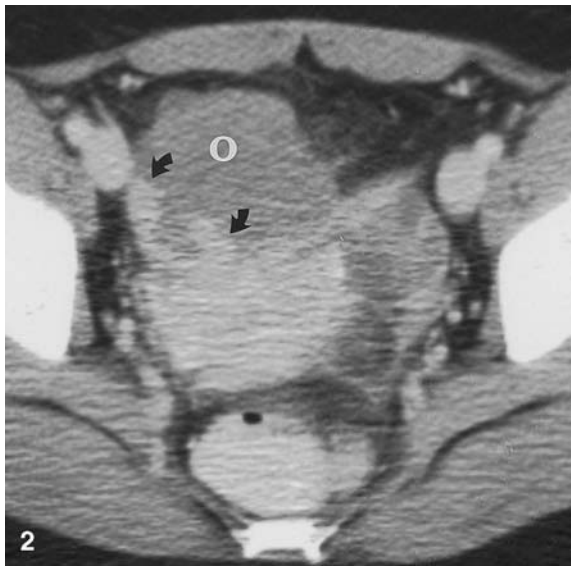

Fig. 1. Ovarian torsion in a 34-year-old female with acute onset of right lower quadrant pain. Endovaginal ultrasound demonstrates an enlarged, edematous ovary containing multiple peripheral hypoechoic follicles. No vascularity was demonstrated on the color or spectral Doppler scans (not shown).

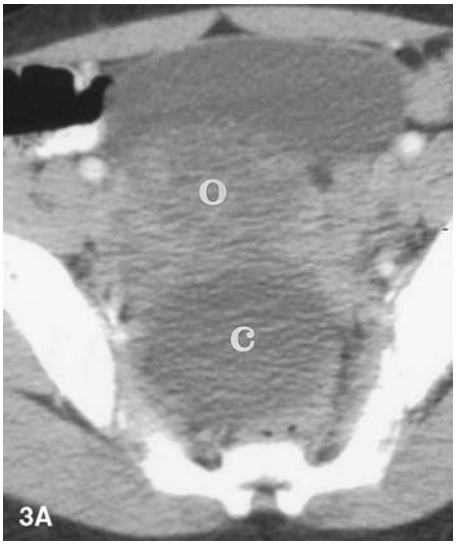

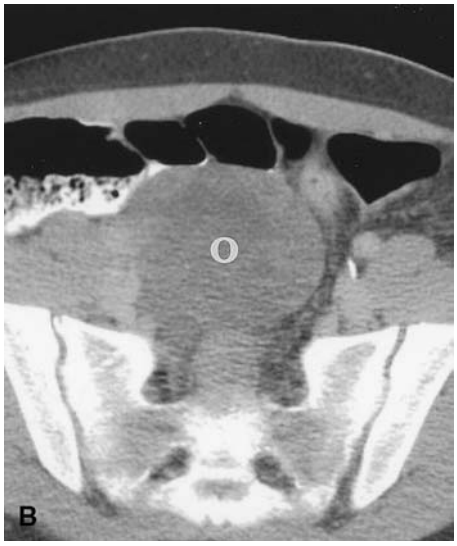

Fig. 2. Ovarian torsion in a 32-year-old female with right lower quadrant pain and a suspected diagnosis of acute appendicitis. Contrast-enhanced CT demonstrates an enlarged right ovary (*O*) displaced anteriorly to the uterus, with a distended vascular pedicle (*arrows*) assuming a beaked configuration at the periphery of the ovary. A normal-appearing left ovary lies adjacent to the uterus.

Fig. 3. Ovarian torsion in a 14-year-old female with acute onset of pelvic pain. **A** Contrast-enhanced CT demonstrates an enlarged left ovary (*O*) that is displaced anteriorly. A large follicular cyst (*C*) is present posteriorly, which served as the fulcrum for torsion. **B** A more cephalad image shows the enlarged, edematous ovary (*O*) with poor enhancement, which proved to be infarcted at surgery.

ripherally distributed follicles, lack of vascularity, and an associated cyst or mass [4–6] (Fig. 1). Occasionally, ultrasound findings are equivocal, and torsion will remain a clinical diagnosis. This may become a diagnostic challenge because torsion may be subacute or intermittent with variable clinical signs. CT may be performed if the diagnosis is initially unsuspected. The CT findings in ovarian torsion have been described [7–9]. These findings include an enlarged, edematous ovary that is displaced from its normal location, with or without an associated mass, an enlarged fallopian tube, and distended engorged blood vessels that often assume a beaked configuration at the periphery of the ovary (Fig. 2). If torsion results in hemorrhagic infarction, there may be lack of contrast enhancement of the ovary, hematoma, or gas (Fig. 3). Reactive inflammatory changes in the pelvic fat and pelvic ascites are frequently observed. The diagnosis should be suggested whenever sequential imaging studies demonstrate rotation of an ovarian mass or component of an ovary [10]. Torsion also should be considered in any female patient with acute pelvic pain and a pelvic mass in whom the normal ovaries cannot be visualized on CT.

Ruptured or hemorrhagic ovarian cyst

Hemorrhage into a functional or physiologic cyst, such as a corpus luteal cyst, often presents as acute onset of pelvic

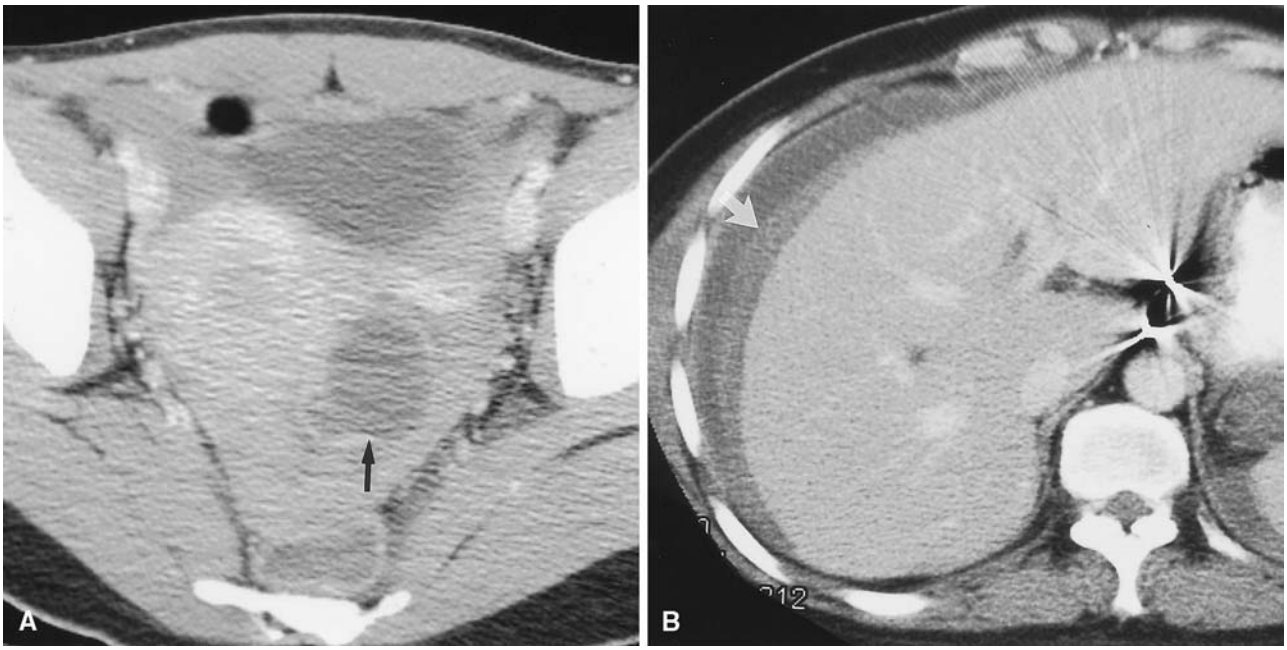

Fig. 4. Ruptured hemorrhagic ovarian cyst in a 28-year-old female who presented with pelvic pain and hypotension. **A** Contrast-enhanced CT shows a large cyst (*arrow*) with peripherally enhancing wall within the left adnexa. Surrounding high attenuation pelvic fluid represents hemoperitoneum. **B** Ascites is present in the abdomen surrounding the liver. High attenuation clot (*arrow*) is present anterior to the liver.

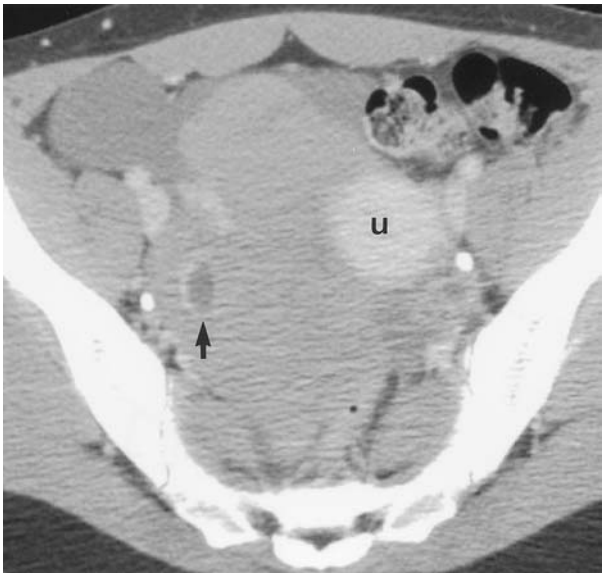

Fig. 5. Ruptured hemorrhagic ovarian cyst in a 30-year-old female with pelvic pain. Contrast-enhanced CT demonstrates the remnant of a ruptured hemorrhagic cyst (*arrow*) with enhancing walls. Surrounding high attenuation material represents hemoperitoneum and clot. *U* uterus

Fig. 6. "Leaking" dermoid in a 41-year-old female with diffuse abdominal and pelvic pain. Contrast-enhanced CT shows a large, midline, cystic pelvic mass with fat peripherally (*arrow*) and a calcification posteriorly. Fluid (*f*) is present in the pelvis secondary to leakage of contents from this benign teratoma. (Courtesy of Dr. Richard D. Gordon.)

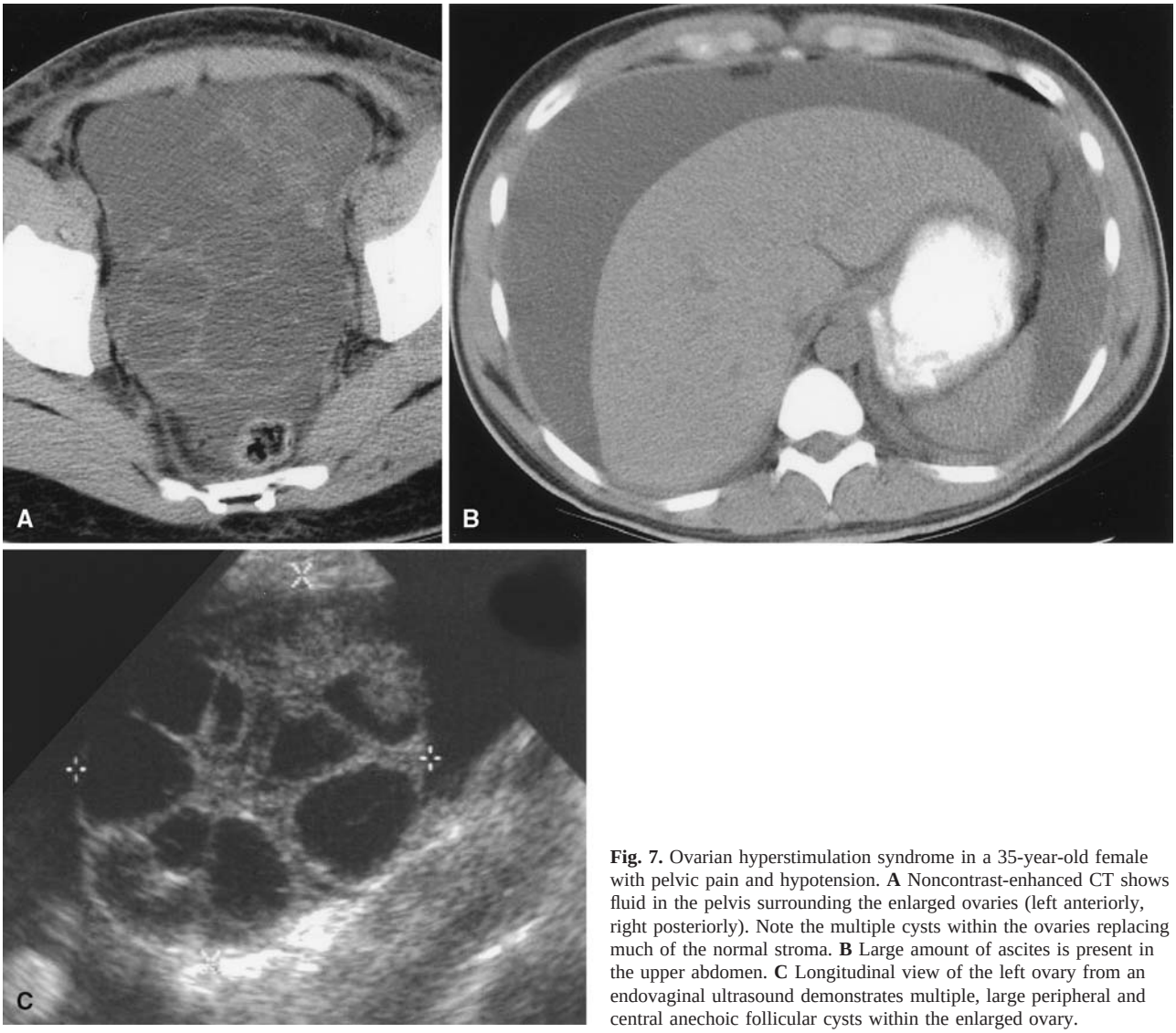

Fig. 7. Ovarian hyperstimulation syndrome in a 35-year-old female with pelvic pain and hypotension. **A** Noncontrast-enhanced CT shows fluid in the pelvis surrounding the enlarged ovaries (left anteriorly, right posteriorly). Note the multiple cysts within the ovaries replacing much of the normal stroma. **B** Large amount of ascites is present in the upper abdomen. **C** Longitudinal view of the left ovary from an endovaginal ultrasound demonstrates multiple, large peripheral and central anechoic follicular cysts within the enlarged ovary.

pain. Corpus luteal cysts are prone to hemorrhage due to the increased vascularity of the ovary during the luteal phase [11]. Rupture of a hemorrhagic ovarian cyst with associated hemoperitoneum can be life-threatening, particularly in patients being treated with anticoagulation therapy [12, 13]. If this is suspected clinically, ultrasound should be the first study of choice, although the cyst may or may not be demonstrated. Findings may include a mass of mixed echogenicity in the adnexa and free fluid corresponding to hemoperitoneum [14]. CT typically reveals hemoperitoneum and an adnexal cyst, with a ring of peripheral contrast enhancement and high attenuation component or fluid–fluid level [12, 15] (Figs. 4, 5). Occasionally, active extravasation of intravenous contrast may be evident if imaging is performed during active bleeding.

On occasion, neoplastic masses may also rupture, although less commonly. The mature cystic teratoma may present with acute pain secondary to rupture with intraperitoneal spillage of cyst contents and associated chemical peritonitis (Fig. 6) [16]. This may lead to fat-containing peritoneal implants [17].

Ovarian hyperstimulation syndrome

Ovarian hyperstimulation syndrome is usually iatrogenic and results from ovarian stimulant drug therapy for infer-

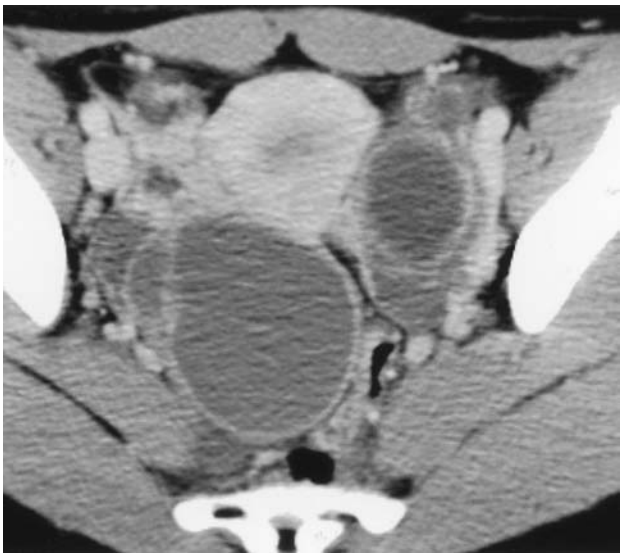

Fig. 8. Endometriomas in a 30-year-old female with pelvic pain. Contrast-enhanced CT demonstrates bilateral, complex adnexal masses with septations.

Fig. 9. Endometriotic implant within the abdominal wall in a 28-year-old female with a history of cesarean section who presented with a palpable, tender abdominal wall mass. Contrast-enhanced CT demonstrates a markedly enhancing soft tissue mass (*arrow*) within the left rectus muscle representing an endometriotic implant. The midline, linear defect in the abdominal wall is the incisional site from prior surgery.

tility causing marked ovarian enlargement with multiple corpora lutea cysts [18]. In addition to ovarian enlargement, this syndrome includes extravascular accumulation of exudates leading to weight gain, ascites, pleural effusions, intravascular volume depletion with hemoconcentration, and oliguria. These patients present with abdominal pain, distention, nausea, and vomiting. The imaging findings are similar on sonography, CT, and magnetic resonance imaging (MRI) [19, 20] and reflect ovarian enlargement by distended corpora lutea cysts of different sizes and ascites (Fig. 7). Familiarity with this syndrome and the appropriate clinical setting should minimize confusion with ovarian cystic neoplasm.

Fig. 10. Small bowel obstruction secondary to endometriotic implant on small bowel wall in a 48-year-old female who presented with nausea and vomiting. Contrast-enhanced CT shows an enhancing soft tissue mass (*arrow*) contiguous with the small bowel, which is dilated and filled with fluid, consistent with small bowel obstruction. At surgery, this mass, initially thought to represent a neoplasm, was shown to represent an endometriotic implant.

Endometriosis

Endometriosis results from the ectopic location of endometrial glands and stroma outside the uterus. This occurs in approximately 10% of women and usually regresses during menopause [21]. The ovary is the most common site of implantation. Other sites include the uterine serosal surface, rectovaginal septum, fallopian tubes, and bowel, most commonly the rectosigmoid colon [22]. Laparoscopy remains the gold standard for diagnosis and staging and is best for identifying small peritoneal implants. Ultrasound is helpful for larger implants. The ultrasound features of endometriotic cysts include a complex cyst with uniform low-level echoes and lack of internal vas-

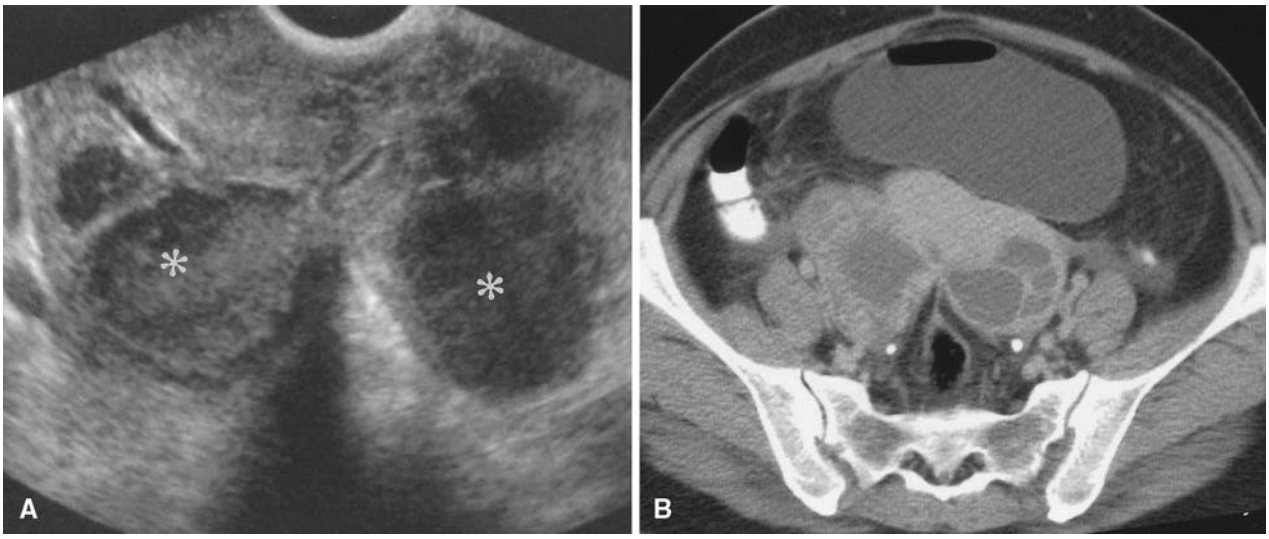

Fig. 11. Tubo-ovarian abscess in a 27-year-old female with pelvic pain and fever who was not responding to a 7-day course of antibiotics. **A** Endovaginal ultrasound shows bilateral, complex adnexal masses (*) with septations, debris, and irregular, thickened walls representing tubo-ovarian abscesses. **B** The corresponding CT demonstrates bilateral, complex adnexal masses that are thick walled and have multiple enhancing septae. Adjacent ascites and inflammatory changes in the pelvic fat are present. Incidental air is noted in the bladder secondary to a Foley catheter not visualized on this image.

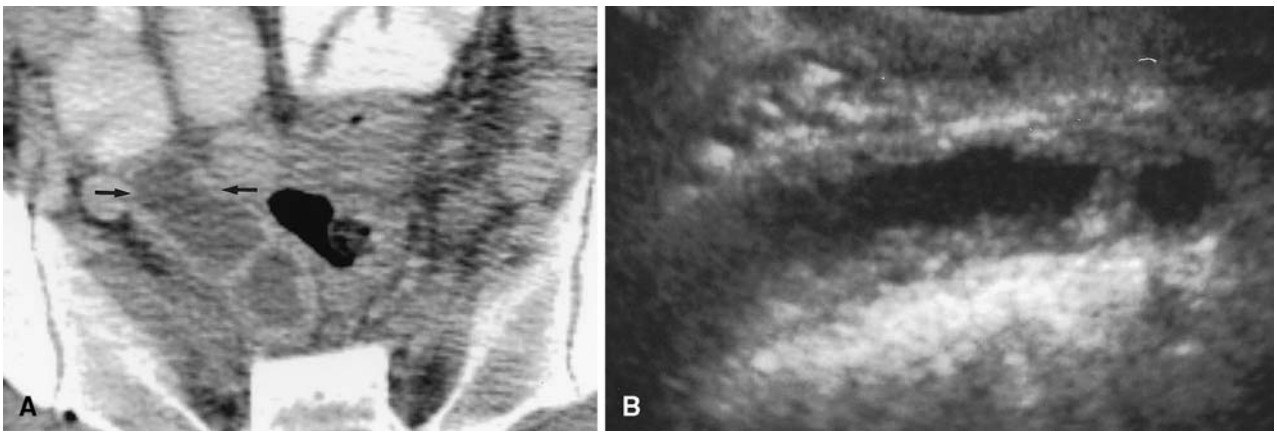

Fig. 12. Salpingitis in a 24-year-old female with right lower quadrant pain and clinically suspected acute appendicitis. **A** Contrast-enhanced CT demonstrates a distended, fluid-filled fallopian tube (*arrows*) with a thickened, enhancing wall. **B** Corresponding endovaginal ultrasound demonstrates a fluid- and debris-filled tubular structure with a thickened, irregular wall, representing the distended, inflamed fallopian tube.

cularity with color Doppler [23–26]. MRI has proven useful in improving the diagnostic specificity when the phenomenon of "shading" is observed [27]. "Shading" refers to the loss of signal intensity on T2-weighted images secondary to high iron and protein concentrations within these lesions.

The CT appearance of endometriomas is nonspecific and includes a spectrum of simple cystic to complex cystic masses [24–26, 28]. At times, a high attenuation component may be evident; however, this is nonspecific because other hemorrhagic lesions, such as hemorrhagic cyst, may demonstrate this finding. Multiple lesions increase the specificity for this diagnosis because endometriomas are often multiple (Fig. 8). CT also may be helpful in staging disease extent and identifying more unusual sites of endometriotic implants including the anterior abdominal wall. This usually occurs at the site of a scar or is related to an amniocentesis needle tract and results from mechanical transplantation of endometrial cells into the abdominal wall. Implants may be contained

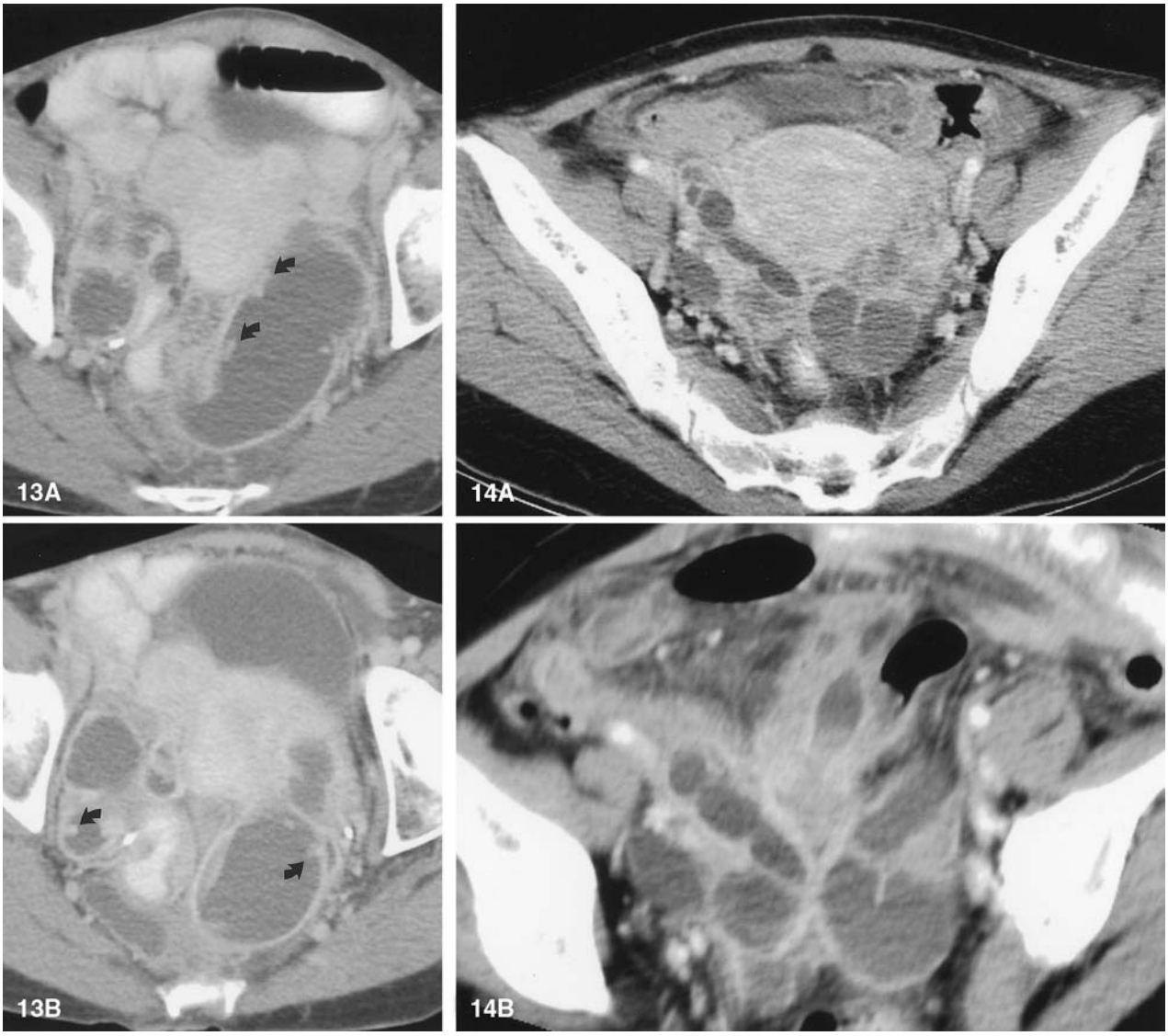

Fig. 13. Bilateral tuboovarian abscesses in a 42-year-old female. **A, B** Sequential axial images from a contrast-enhanced CT show complex cystic masses within the pelvis representing tubo-ovarian abscesses. Note the fluid-filled fallopian tubes demonstrating thickened endosalpingeal folds (*arrows*), which aided the diagnosis.

Fig. 14. Tubo-ovarian abscess in a 37-year-old female with pelvic pain and fever. **A** Initial axial image from a contrast-enhanced CT demonstrates bilateral, enhancing, complex cystic masses posterior to the uterus. **B** A coronal reformatted image demonstrates the tubular nature of these masses, helping to diagnose them as tubo-ovarian abscesses.

within the rectus muscle or extend into the subcutaneous soft tissues [29, 30]. Cyclical pain due to monthly ovulatory hormonal influences suggests the diagnosis. Clinically, a peri-incisional abdominal wall hernia may be suspected. On CT, such an endometriotic implant appears as a mass within the anterior abdominal wall that demonstrates marked contrast enhancement [31] (Fig. 9). The differential diagnosis includes other soft tissue masses such as a desmoid tumor or hypervascular metastases. An additional unusual site of implantation is the small bowel, which may result in small bowel obstruction and simulate small bowel neoplasm (Fig. 10). In such cases, other CT findings of endometriosis or characteristic clinical history may help to suggest endometriosis as the etiology.

Pelvic inflammatory disease

Pelvic inflammatory disease (PID) results from ascending infection of the genital tract and is usually polymicrobial in nature with a mixture of anaerobes and aerobes. This

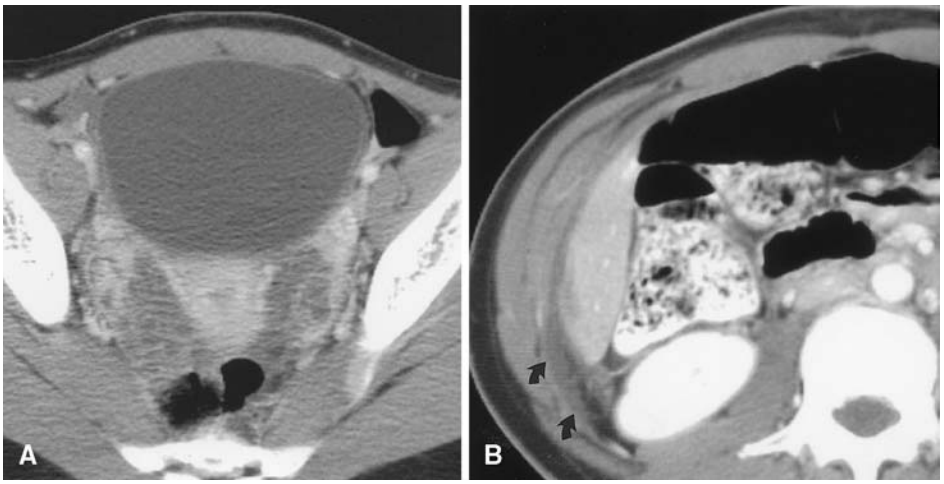

Fig. 15. Fitz-Hugh-Curtis syndrome in a 28-year-old female with PID and right upper quadrant pain. **A** Contrast-enhanced CT shows bilateral salpingitis with thickened and distended tubes. **B** Enhancement and soft tissue stranding of the perihepatic fat (*arrows*) represents spread of inflammation from PID.

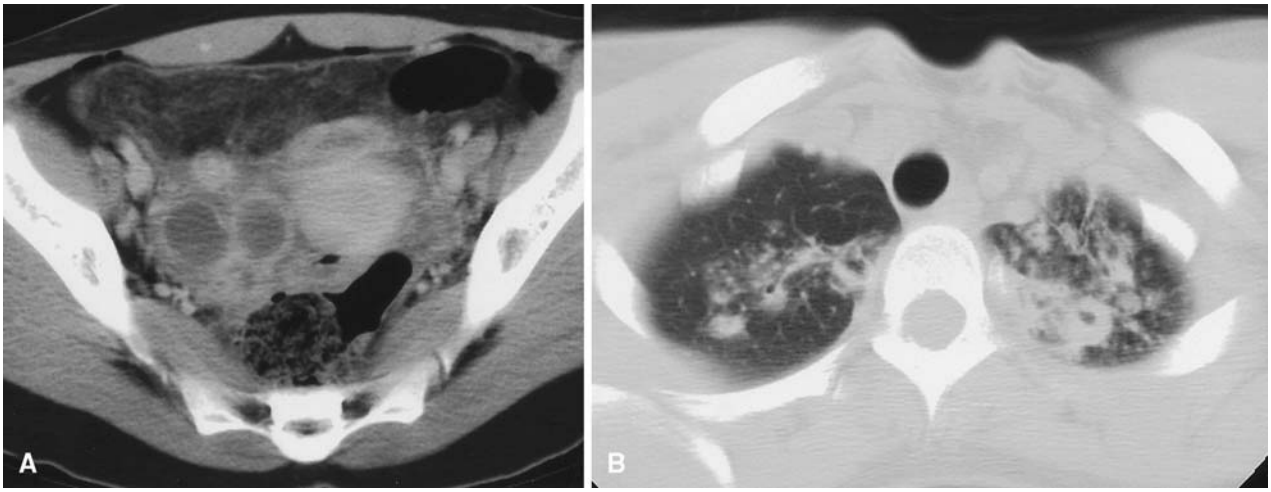

Fig. 16. PID secondary to tuberculosis in a 30-year-old female with chronic pelvic pain. **A** Contrast-enhanced CT demonstrates a complex, cystic adnexal mass on the right. There are extensive inflammatory changes, with thickening of the peritoneum and omentum simulating carcinomatosis. **B** An image from concurrent chest CT helps identify the true etiology of the pelvic findings. Biapical cavitary nodules with surrounding consolidation result from tuberculosis infection.

begins as endometritis, which progresses to salpingitis and ultimately tubo-ovarian abscess. Ultrasound, in conjunction with clinical history and findings, is usually diagnostic. The spectrum of findings may range from hydro- or pyosalpinx to tubo-ovarian complex, where the architecture of the ovary is preserved, to tubo-ovarian abscess. The tubo-ovarian abscess appears as a complex, solid and cystic mass with complete destruction of the architecture of the ovary, which can no longer be delineated (Fig. 11A).

In the setting of PID, CT is most useful when clinical and ultrasound evaluations are difficult to perform or equivocal, when patients fail to respond to antibiotic therapy, to stage the full extent of the inflammatory process, and to detect complications such as abscess and septic thrombophlebitis. On CT, the imaging findings differ with the stage of disease and may overlap with other inflammatory processes or even neoplasm [25, 32, 33]. Findings are usually bilateral, although one side may be affected more than the other. Initially, salpingitis may appear as a thickened, dilated fallopian tube. On ultrasound and CT, the presence of mural nodules corresponding to thickened endosalpingeal folds helps to identify this structure as the fallopian tube and differentiates it

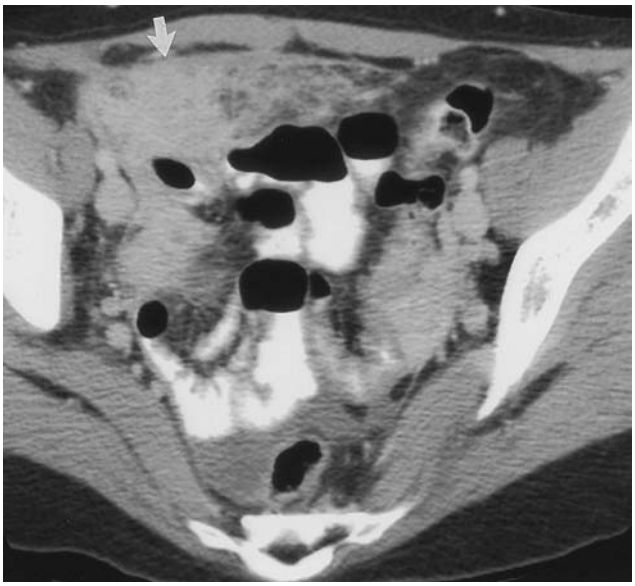

Fig. 17. PID secondary to actinomycosis in a 35-year-old female with an IUD in place. Contrast-enhanced CT demonstrates extensive inflammatory changes within the pelvis, with thickening of the peritoneum and infiltration of the omentum (*arrow*). Although this could represent carcinomatosis, the true etiology is PID secondary to actinomycosis in this patient with an IUD (not visualized on this image).

Fig. 18. Leiomyomas in a 45-year-old female. Contrast-enhanced CT demonstrates dense, confluent masses with different degrees of enhancement deforming the uterine contour consistent with multiple subserosal fibroids (*f*). Several calcifications are seen on the right (*arrow*), not an infrequent finding.

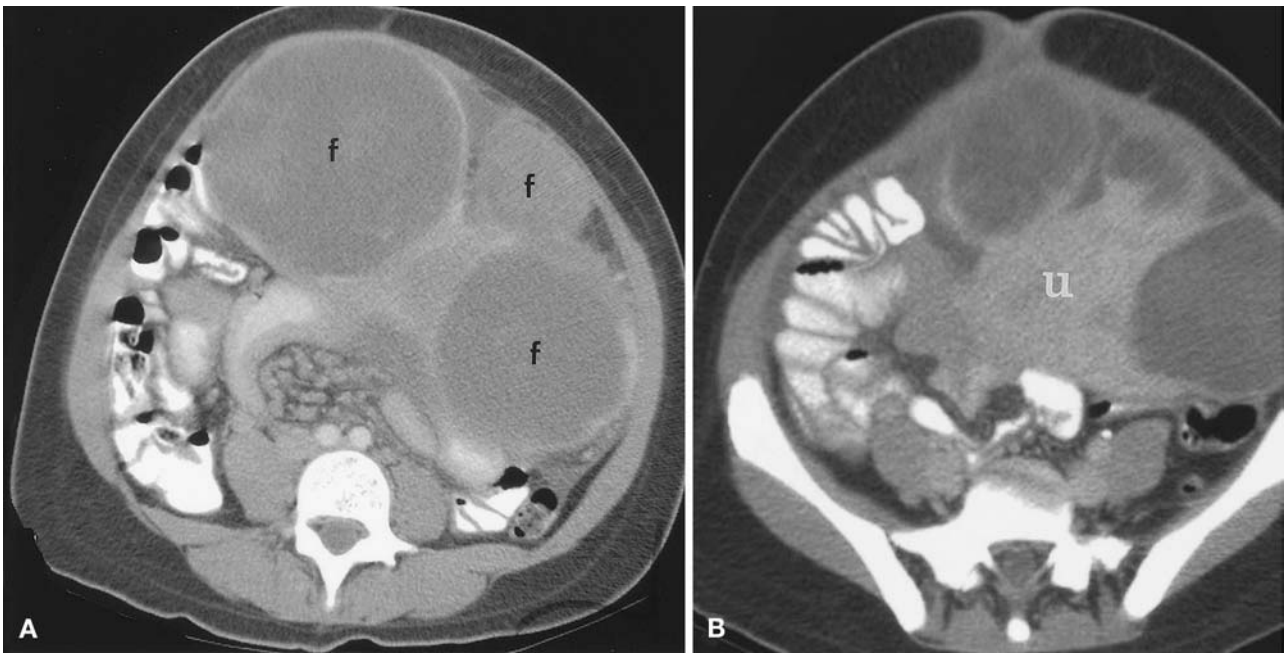

Fig. 19. Leiomyomas in a patient with a large, palpable abdominal and pelvic mass who presented with pelvic pain. **A** Contrast-enhanced CT shows three subserosal fibroids (*f*) that are low attenuation secondary to cystic degeneration. **B** At a more caudal level, areas of high attenuation are present, representing hemorrhagic infarction. *u* uterus.

Fig. 20. Pedunculated, infarcted leiomyoma with coarse calcification in a 50-year-old postmenopausal female with pelvic pain. Contrast-enhanced CT shows a pedunculated fibroid with diminished attenuation relative to the uterus (*u*) secondary to infarction. The rim of the fibroid is calcified, and a central nidus of calcification is also present.

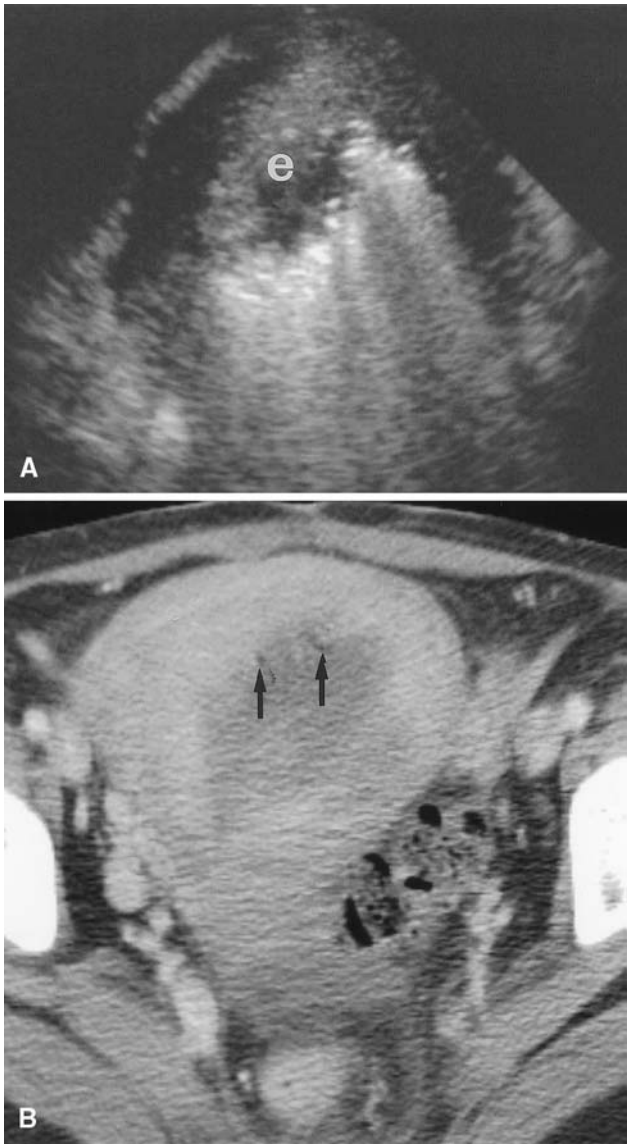

Fig. 21. Endometritis in a 28-year-old female with postpartum fever. **A** An axial image from an endovaginal ultrasound shows the thickened endometrium (*e*) containing fluid. Hyperechoic material with shadowing represents gas. **B** Contrast-enhanced CT also demonstrates that the endometrial canal is filled with fluid and distended and contains small foci of air (*arrows*).

from the inflamed appendix, which may occasionally be located in the region of the adnexa (Fig. 12). Tubo-ovarian abscess appears as a complex cystic mass with enhancing thickened septations (Figs. 11B, 13). Recognition of the tubular nature of the mass helps to identify it as a tubo-ovarian abscess. This can be facilitated with the use of multiplanar reformations. (Fig. 14). Other associated findings include thickening of the broad ligament and uterosacral ligaments, loss of definition of the uterine border, infiltration of the pelvic fat, and reactive lymphadenopathy. Occasionally, spread of inflammation to the perihepatic tissues may be visualized, corresponding to the clinical findings of perihepatitis, known as Fitz-Hugh-Curtis syndrome [34] (Fig. 15).

Two atypical organisms that may cause PID include tuberculosis and actinomycosis. Genitourinary tuberculosis usually presents as a chronic indolent infection, often with infertility as the presenting problem. Infection is usually secondary to hematogenous spread from pulmonary or other nongenital tract foci [35]. The fallopian tubes and endometrium are the most common sites of involvement. There may be associated ascites and peritonitis, which may be difficult to distinguish from carcinomatosis [36] (Fig. 16). The diagnosis can be confirmed by histology that reveals typical granulomas or acid fast stain or culture of the surgical specimen.

Actinomycosis israelli is a gram-positive nonacid-fast anaerobic bacterium usually found in the gastrointestinal tract. This is a rare cause of indolent pelvic infection. Infection may be secondary to hematogenous spread from another source, or ascending infection that occurs in the setting of an intrauterine device (IUD). Colonization of

the lower genital tract occurs most often in the presence of an IUD or other foreign body and increases with the duration of IUD use [37]. By the time the patient seeks treatment, the pelvic organs may be massively indurated and fibrotic with destruction and adherence to surrounding structures. Invasion across tissue planes may lead to ureteric obstruction or colonic stricture [38]. Due to the dense inflammatory response and contrast enhancement of the solid component, infection with this organism may be difficult to distinguish from pelvic neoplasm and carcinomatosis [39] (Fig. 17).

The uterus

Fibroids

Fibroids, or leiomyomas, are the most common disorder of the uterus and occur in more than 20% of women older than 30 years [40, 41]. Ultrasound is usually diagnostic, and CT is not recommended for primary evaluation. However, because fibroids are so common, it is important to become familiar with their CT appearance. CT findings will depend on the presence of intravenous contrast, size and location of fibroids, and degree of degeneration. The fibroid uterus is enlarged with lobulated contour and heterogeneous attenuation. Fibroids appear as a focal masses that may be submucosal, intramural, or subserosal in location (Fig. 18). The degree of contrast enhancement often will vary with the extent of degeneration. Regions of degeneration typically demonstrate less enhancement and low attenuation components [42, 43] (Fig. 19). Enhancement characteristics also will depend on the timing of imaging with respect to the phase of the contrast bolus. During the arterial phase, there may be areas that demonstrate brisk enhancement and become isoattenuating on more delayed images. Occasionally, it is difficult to distinguish a submucosal fibroid from endometrial pathology, or a pedunculated fibroid from adnexal pathology. In this setting, sonohysterography or MRI may be helpful for further evaluation [44–46]. On CT, the presence of coarse calcifications may help to suggest pathology of uterine origin [47] (Fig. 20). Unfortunately, in the absence of clear extrauterine extension or metastatic disease, differentiation between large, benign complicated fibroids and leiomyosarcoma may not always be possible.

Endometritis

Endometritis usually occurs in the postpartum setting and is the most common cause of fever in the postpartum patient, with a reported prevalence of 3.8% [48]. This is associated with prolonged labor, premature rupture of membranes, retained clot, and retained products of conception. Endometritis occasionally can occur in the setting of cervical stenosis or after instrumentation. This diagnosis is usually made on clinical grounds in the setting of fever and an enlarged, tender uterus. Endometritis may progress to myometritis and be complicated by salpingitis, pelvic abscess, and septic thrombophlebitis. Imaging is performed when the patient does not respond to conventional therapy. The imaging findings are similar on CT and ultrasound and include fluid and debris within the distended endometrial cavity [49–52] (Fig. 21). It is important to remember that air may be present in the uterine cavity up to 6 weeks after normal vaginal delivery and that the presence of air alone is not diagnostic [53]. CT is complementary to ultrasound for identifying complications such as pelvic abscess or septic thrombophlebitis. Retained products of conception are diagnosed when there is material within the uterine cavity, which demonstrates vascularity with color Doppler ultrasound or contrast enhancement on CT [52] (Fig. 22).

Fig. 22. Retained products of conception in a 30-year-old postpartum patient presenting with vaginal bleeding. Contrast-enhanced CT demonstrates a distended endometrial canal containing fluid and heterogeneous, enhancing material (*arrow*) representing retained products of conception.

Uterine perforation or rupture

This is an uncommon disorder that is usually iatrogenic in nature and related to procedures such as dilatation and

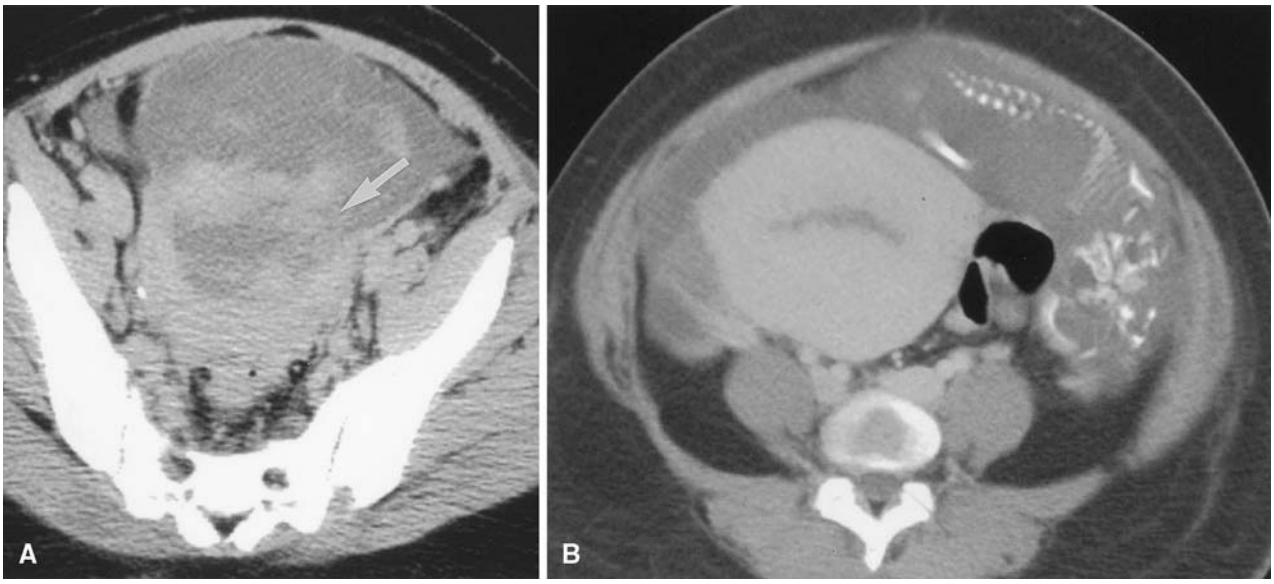

Fig. 23. Uterine rupture in a pregnant patient with a history of cesarean section who was started on Pitocin and subsequently developed intense abdominal pain. **A** Contrast-enhanced CT demonstrates a site of uterine rupture on the left (*arrow*). **B** A more cephalad image demonstrates the fetus extruded into the peritoneal cavity.

Fig. 24. Post–cesarean section uterus. Contrast-enhanced CT in a patient with previous cesarean section demonstrates the postoperative appearance of the uterus. Note continuity of the serosal surface (*arrows*) and high attenuation material in the anterior uterine wall representing hematoma.

curettage or long-standing IUD usage. Uterine rupture occasionally can occur in the setting of the gravid uterus, and patients who have undergone prior uterine surgery, including cesarean section, myomectomy, or prolonged or induced labor, are at risk [54]. Although this diagnosis may be made on ultrasound, CT offers the advantage of visualizing the parametrial structures and associated complications such as abscess (Fig. 23).

Postoperative and postpartum complications

CT is the primary imaging modality of choice for postoperative complications such as pelvic abscess and hematoma. Uterine perforation may result from dilatation and curettage or may occasionally occur during pregnancy, as discussed above. A hematoma in the anterior wall of the uterus may occur after cesarean section and appears as an area of decreased attenuation with the serosal contour intact [55] (Fig. 24). In contrast, dehiscence of cesarean section scar (Fig. 25) is diagnosed on CT as a disruption of the uterine contour, often with associated abscess [51, 52].

Ovarian vein thrombosis (OVT) frequently occurs in the postpartum setting but may also occur after pelvic surgery or as a complication of inflammatory conditions of the pelvis, such as endometritis or PID [56–58]. OVT has an overall incidence of 1 in 3000 deliveries [59]. In 80–90% of cases, the right ovarian vein is involved. This predilection for right-sided involvement most likely results from the fact that the left ovarian vein drains into the left renal vein and retrograde flow prevents venous stasis on the left [51]. In a comparative study by Twickler et al. [60], contrast-enhanced CT and MRI were shown to have greater sensitivity and specificity than Doppler ultrasound in the detection of OVT. On contrast-enhanced CT, the vein may appear distended and contain an intralumenal filling defect corresponding to thrombus, or there may be complete lack of enhancement of the vein (Fig. 26). There is usually associated inflammatory change in the pelvic fat or ascites. Diagnostic pitfalls include the inflamed

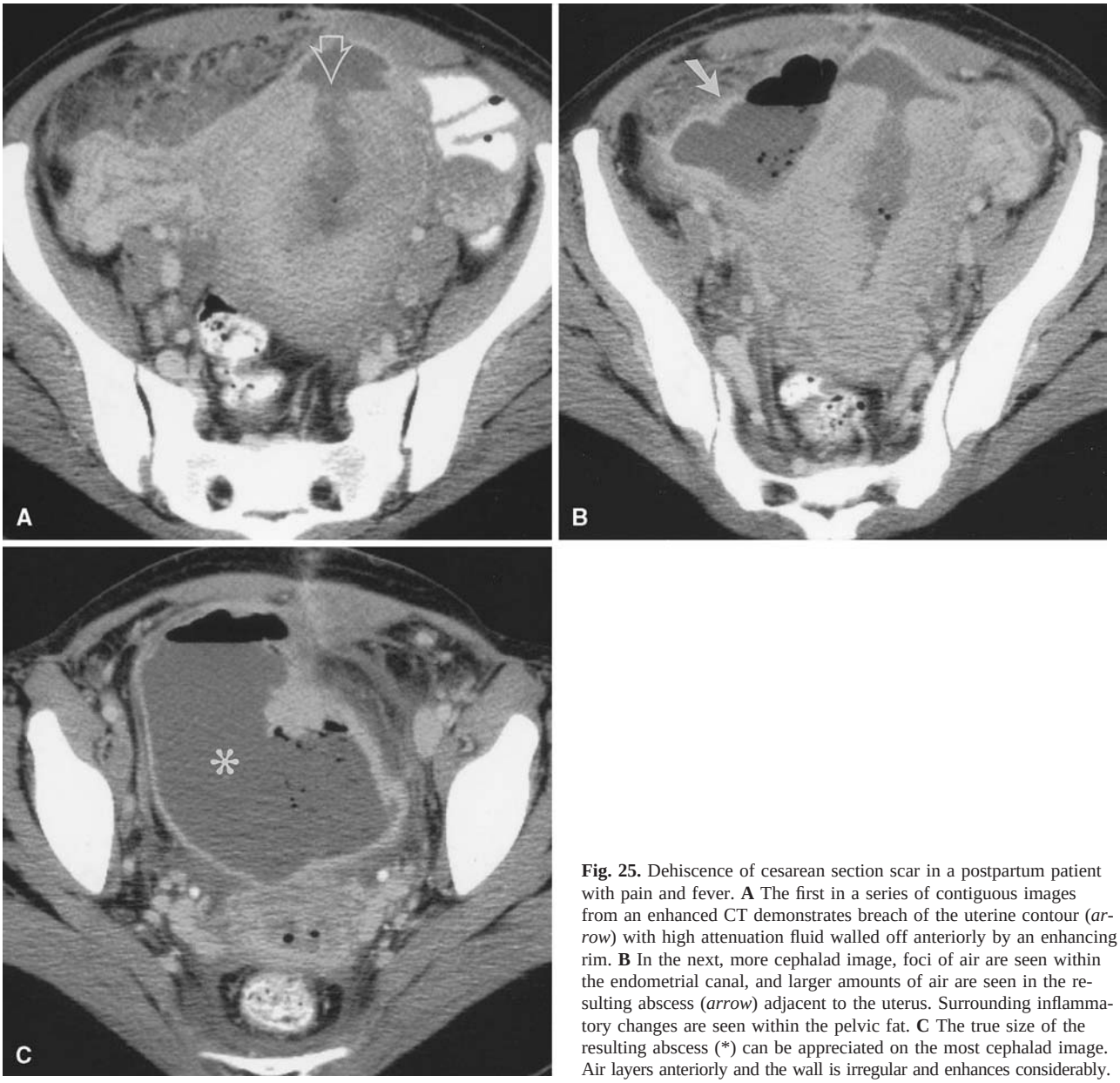

Fig. 25. Dehiscence of cesarean section scar in a postpartum patient with pain and fever. **A** The first in a series of contiguous images from an enhanced CT demonstrates breach of the uterine contour (*arrow*) with high attenuation fluid walled off anteriorly by an enhancing rim. **B** In the next, more cephalad image, foci of air are seen within the endometrial canal, and larger amounts of air are seen in the resulting abscess (*arrow*) adjacent to the uterus. Surrounding inflammatory changes are seen within the pelvic fat. **C** The true size of the resulting abscess (*) can be appreciated on the most cephalad image. Air layers anteriorly and the wall is irregular and enhances considerably.

appendix or dilated ureter, both of which are also tubular structures with central nonenhancement [61]. Careful inspection over sequential images usually helps to avoid this problem because the inflamed appendix can be followed to the base of the cecum and the dilated ureter back to the hydronephrotic kidney. If unrecognized and left untreated, OVT may result in septic pulmonary emboli (Fig. 27).

HELLP (hemolysis, elevated liver enzymes, and low platelets) syndrome occurs in 4–12% of preeclamptic patients [62–64]. This syndrome results from toxemia-related vascular endothelial injury, which causes intravascular deposition of fibrin and end organ damage. This can occur before or after delivery. Major complications of this syndrome include disseminated intravascular coagulation, placental abruption, acute renal failure, pulmonary edema, pleural and pericardial effusions and hepatic infarction, hematoma, and rupture. Spontaneous intrahepatic hemorrhage and rupture present as acute right upper quadrant pain and hypotension (Fig. 28). CT is important in initial diagnosis and for serial follow-up [65]. Findings may include subcapsular and intrahepatic hemorrhages,

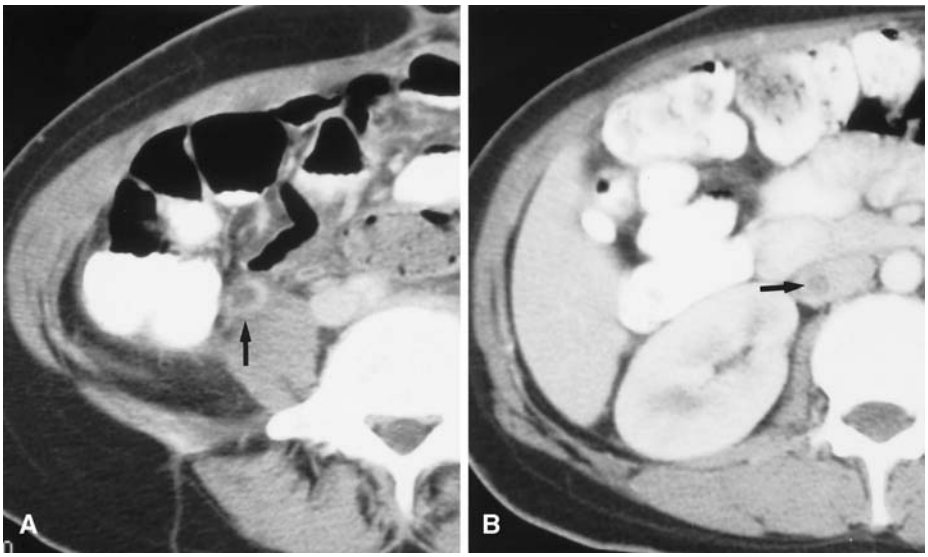

Fig. 26. OVT in a 25-year-old female status post dilatation and curettage. **A** Contrast-enhanced CT shows an enlarged right ovarian vein (*arrow*) with central low attenuation thrombus. This could easily be mistaken as appendicitis if sequential images are not inspected to trace the vein along its course. **B** More cephalad, the thrombus (*arrow*) is seen to extend into the inferior vena cava.

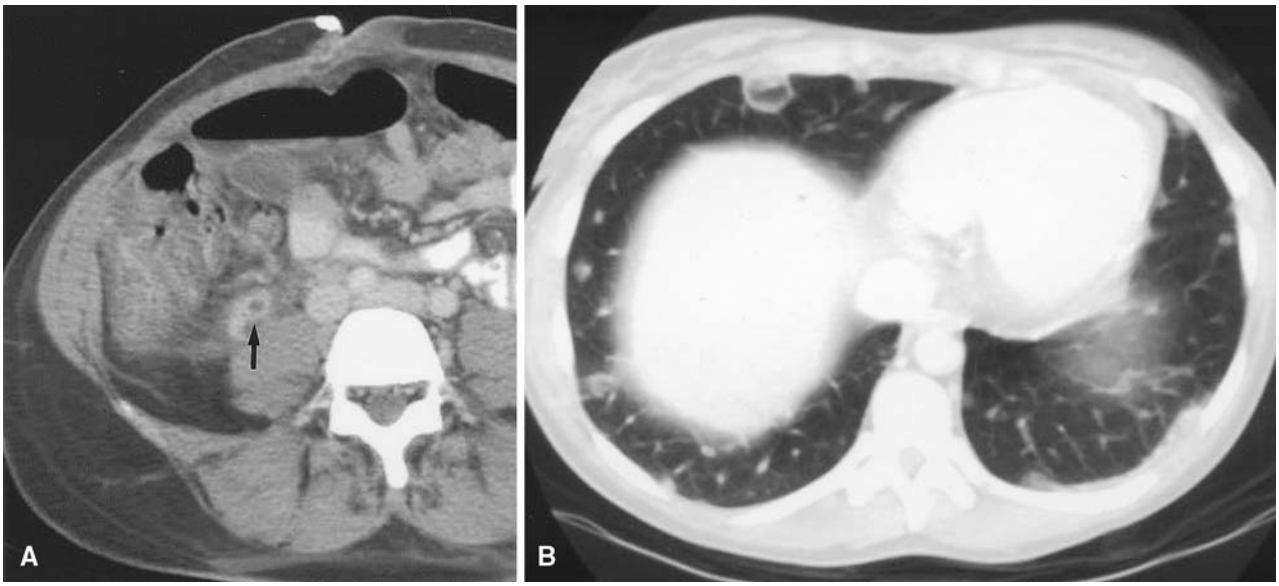

Fig. 27. OVT in a young patient with PID. **A** Contrast-enhanced CT shows low attenuation in the right ovarian vein (*arrow*) with associated inflammatory changes. **B** The patient complained of dyspnea, and chest CT demonstrates multiple, peripheral, cavitary nodules consistent with septic emboli.

capsular rupture, and areas of confluent necrosis secondary to infarction. CT with intravenous contrast may demonstrate active arterial extravasation, which may be amenable to transcatheter embolization.

Inflammatory disorders of the bowel that may secondarily involve the adnexa

Acute appendicitis and diverticulitis may secondarily involve the adnexa. The appendix may extend into the right adnexa, sometimes between the ovary and the uterus (Fig. 29), and when inflamed appears as a thick-walled enhancing tubular fluid-filled structure. This can at times be difficult to distinguish from primary adnexal pathology such as salpingitis. Over sequential images, it usually will be apparent that this structure arises from the base of the cecum, with associated cecal thickening. An appendicolith is another very helpful finding. Visualization of thickened endosalpingeal folds is characteristic of tubal pathology. Acute diverticulitis can involve the right or left colon, although most

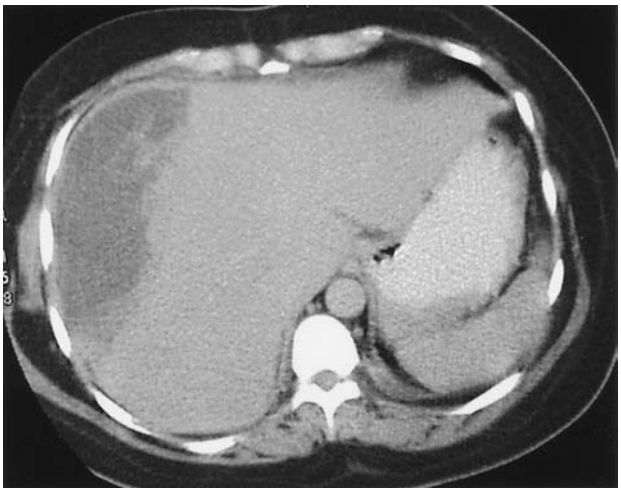

Fig. 28. Complications of HELLP syndrome. Contrast-enhanced CT was performed on a 34-year-old woman postpartum day 3 who presented with right upper quadrant pain. The scan demonstrates a subcapsular hepatic hematoma.

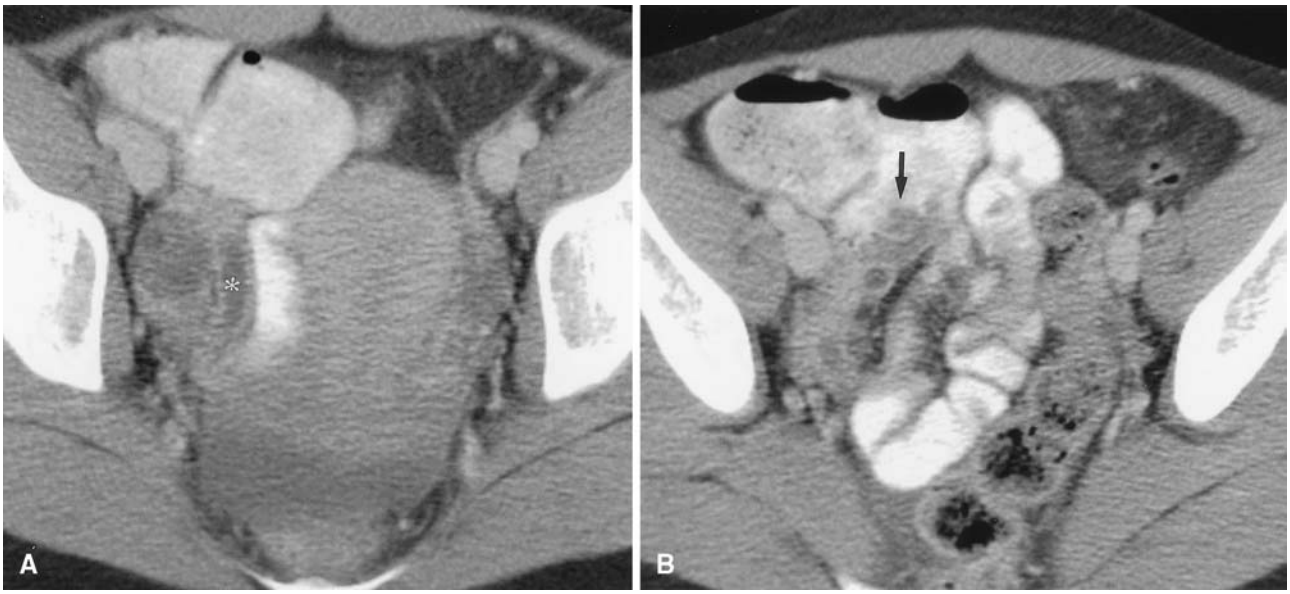

Fig. 29. Acute appendicitis in a 17-year-old female with right lower quadrant pain. **A** Contrast-enhanced CT shows a distended, tubular structure (*) interposed between the uterus and right ovary, representing an inflamed appendix. **B** A more cephalad image demonstrates the origin of the structure arising from the base of the cecum, which is thickened (*arrow*), helping to establish this as appendicitis.

commonly involves the sigmoid colon. A diverticular abscess may involve the adnexa. The identification of an inflamed diverticulum helps to confirm diverticulitis as the etiology (Fig. 30).

Disorders of an ectopic kidney in the pelvis may present as acute pelvic pain and clinically mimic primary adnexal pathology. At times, the hydronephrotic kidney on ultrasound may simulate a complex cystic adnexal mass, and this pitfall should be considered. In such cases, CT can be helpful in delineating a mass as a hydronephrotic pelvic kidney and may help to identify the etiology of obstruction, such as a calculus (Fig. 31).

Conclusion

Many acute gynecologic disorders that cause abdominal or pelvic pain demonstrate characteristic findings on CT. As CT continues to play an ever increasingly important role in the evaluation of the patient who presents with abdominal and pelvic pain, the radiologist must become familiar with these findings. This may eliminate the need for additional imaging and help to guide appropriate patient management. CT is complementary to ultrasound and may enable improved characterization of inflammatory disorders and more accurate staging of disease extent.

Fig. 30. Diverticular abscess in a 60-year-old female with left lower quadrant pain. Contrast-enhanced CT shows thickening of the wall of the sigmoid colon with inflammatory changes in the adjacent fat secondary to diverticulitis. Several small diverticula are seen in the sigmoid. An adjacent complex, cystic mass containing air represents abscess formation (*). Although this is within the left adnexal region, other findings suggest diverticulitis with abscess formation rather than a primary adnexal process.

Fig. 31. Pelvic kidney with hydronephrosis in a patient with left pelvic pain. Contrast-enhanced CT demonstrates a pelvic kidney (*arrow*) that is hydronephrotic secondary to obstructing stones not visualized on this image. Perinephric stranding of the fat is also present.

Acknowledgments. The authors thank Drs. Giovanna Giovaniello, Michael Macari, Kevin Roche, and Morton Bosniak for contribution of case material.

References

1. Kaur H, Loyer EM, Minami M, Charnsangavej C. Patterns of uterine enhancement with helical CT. *Eur J Radiol* 1998;28:250–255
2. Houry D, Abbott JT. Ovarian torsion: a fifteen year review. *Ann Emerg Med* 2001;38:156–159
3. Demopoulos RI, Bigelow B, Vasa U. Infarcted uterine adnexa. Associated pathology. *N Y State J Med* 1978;78:2027–2029
4. Helvie MA, Silver TM. Ovarian torsion: sonographic evaluation. *J Ultrasound Med* 1989;17:327–332
5. Lee EJ, Kwon HC, Joo HJ, et al. Diagnosis of ovarian torsion with color Doppler sonography: depiction of twisted vascular pedicle. *J Ultrasound Med* 1998;17:83–89
6. Wilms AB, Schlund JF, Meyer WR. Endovaginal ultrasound in ovarian torsion: a case series. *Ultrasound Obstet Gynecol* 1995;5:129
7. Kimura I, Togashi K, Kawakami S, et al. Ovarian torsion: CT and MR imaging appearances. *Radiology* 1994;190:337–341
8. Bellah RD, Griscom NT. Torsion of normal uterine adnexa before menarche: CT appearance. *AJR* 1989;152:123–124
9. Kawahara Y, Fukuda T, Futagawa S, et al. Intravascular gas within an ovarian tumor: a CT sign of ovarian torsion. *J Comput Assist Tomogr* 1996;20:154–156
10. Ghossain MA, Buy JN, Sciot C, et al. CT findings before and after adnexal torsion: Rotation of a focal solid element of a cystic mass as an adjunctive sign in diagnosis. *AJR* 1997;169:1343–1346
11. Raziel A, Ron-El R, Pansky M, et al. Current management of ruptured corpus luteum. *Eur J Obstet Gynecol Reprod Biol* 1993;13:549–555
12. Wilbur AC, Goldstein LD, Prywitch BA. Hemorrhagic ovarian cysts in patients on anticoagulation therapy: CT findings. *J Comput Assit Tomogr* 1993;17:623–625
13. Hallatt JG, Steele CH Jr, Snyder M. Rupture corpus luteum with hemoperitoneum: a study of 173 surgical cases. *Am J Osbtet Gynecol* 1984;149:5–9
14. Baltarowicz OH, Kurtz AB, Pasto ME, et al. The spectrum of sonographic findings in hemorrhagic ovarian cyst. *AJR* 1987;148:901–905
15. Hertzberg BS, Kliewer MA, Paulson EK. Ovarian cyst rupture causing hemoperitoneum: imaging features and the potential for misdiagnosis. *Abdom Imaging* 1999;24:304–308
16. Ayhan A, Aksu T, Develioglu O, et al. Complications and bilaterality of mature ovarian teratomas (clinicopathological evaluation of 286 cases). *Aust N Z J Obstet Gynecol* 1991;31:83–85
17. Lindbichler F, Raith J, Tillich M, et al. CT findings in postoperative subphrenic abscess with teratomatous inclusions. *Br J Radiol* 2000;73:542–543
18. Schenker JG, Polishuk WZ. Ovarian hyperstimulation syndrome. *Obstet Gynecol* 1975;46:23–28
19. Kim IY, Lee BH. Ovarian hyperstimulation syndrome: US and CT appearances. *Clin Imaging* 1997;21:284–286
20. Jung BG, Kim H. Severe ovarian hyperstimulation syndrome with MR findings. *J Comput Assist Tomogr* 2001;25:215–217
21. Olive DL, Schwartz LB. Endometriosis. *N Engl J Med* 1993;328:1759–1769
22. Yantiss RK, Clement PB, Young RH. Endometriosis of the intestinal tract: a study of 44 cases of a disease that may cause diverse challenges in clinical and pathological evaluation. *Am J Surg Pathol* 2001;25:445–454
23. Patel MD, FeldsteinVA, Chen DC, et al. Endometriomas: diagnostic performance of US. *Radiology* 1999;210:739–745

24. Woodward PJ, Sohaey R, Mezzetti TP. Endometriosis: radiologic–pathologic correlation. *Radiographics* 2001;21:193–216
25. Langer JE, Dinsmore BJ. Computed tomographic evaluation of benign and inflammatory disorders of the female pelvis. *Radiol Clin North Am* 1992;30:831–842
26. Umaria N, Olliff JF. Imaging features of pelvic endometriosis. *Br J Radiol* 2001;74:556–562
27. Togashi K, Nishimura K, Kimura I, et al. Endometriotic cysts: diagnosis with MR imaging. *Radiology* 1991;180:73–78
28. Buy JN, Ghossain MA, Mark AS, et al. Focal hyperdense areas in endometriomas: a characteristic finding on CT. *AJR* 1992;159:769–771
29. Dwivedi AJ, Agrawal SN, Silva YJ. Abdominal wall endometriomas. *Dig Dis Sci* 2002;47:456–461
30. Patterson GK, Winburn GB. Abdominal wall endometriomas: report of eight cases. *Am Surg* 1999;65:36–39
31. Coley BD, Casola G. Incisional endometrioma involving the rectus abdominis muscle and subcutaneous tissues: CT appearance. *AJR* 1993;160:549–550
32. Wilbur AC, Aizenstein RI, Napp TE. CT findings in tuboovarian abscess. *AJR* 1992;158:575–579
33. Ellis JH, Francis IR, Rhodes M, et al. CT findings in tuboovarian abscess. *J Comput Assist Tomogr* 1991;4:589–592
34. Romo LV, Clarke PD. Fitz-Hugh-Curtis syndrome: pelvic inflammatory disease with an unusual CT presentation. *J Comput Assist Tomogr* 1992;16:832–833
35. Ryan KJ, Berkowitz RS, Barbieri RL, Dunaif A, eds. *Kistner's gynecology and women's health*, 7th ed. St Louis: Mosby, 1999:462
36. Bilgin T, Karabay A, Dolar E, Develioglu OH. Peritoneal tuberculosis with pelvic abdominal mass, ascites and elevated CA 125 mimicking ovarian carcinoma: a series of 10 cases. *Int J Gynecol Cancer* 2001;11:290–294
37. Maenpaa J, Taina E, Gronroos M, et al. Abdominopelvic actinomycosis associated with intrauterine devices. Two case reports. *Arch Gynecol Obstet* 1988;243:237–241
38. Hochsztein JG, Koenigsberg M, Green DA. US case of the day. Actinomycotic pelvic abscess secondary to an IUD with involvement of the bladder, sigmoid colon, left ureter, liver and upper abdominal wall. *Radiographics* 1996;16:713–716
39. Hinnie J, Jacques BC, Bell E, et al. Actinomycosis presenting as carcinoma. *Postgrad Med J* 1995;71:749–750
40. Zaloudek C, Norris HJ. Mesenchymal tumors of the uterus. In: Kurman RJ, ed. *Blaustein's pathology of the female genital tract.* New York: Springer-Verlag, 1994:487–498
41. Silverberg SG, Kurman RJ. Smooth muscle and other mesenchymal tumors. In: Rosai J, ed. *Tumors of the uterine corpus and gestational trophoblastic disease, fasc 3, ser 3.* Washington, DC: Armed Forces Institute of Pathology, 1992:113–130
42. Ueda H, Togashi K, Konishi I, et al. Unusual appearances of uterine leiomyomas: MR imaging findings and their histopathologic backgrounds. *Radiographics* 1999;19:S131–S145
43. Murase E, Siegelman ES, Outwater EK, et al. Uterine leiomyomas: histopathologic features, MR imaging findings, differential diagnosis, and treatment. *Radiographics* 1999;19:1179–1197
44. Jorizzo JR, Riccio GJ, Chen MY, Carr JJ. Sonohysterography: the next step in the evaluation of the abnormal endometrium. *Radiographics* 1999;19:S117–S130
45. Weinreb JC, Barkoff ND, Megibow A, Demopoulos R. The value of MR imaging in distinguishing leiomyomas from other solid pelvic masses when sonography is indeterminate. *AJR* 1990;154:295–299
46. Kim JC, Kim SS, Park JY. "Bridging vascular sign" in the MR diagnosis of exophytic uterine leiomyoma. *J Comput Assist Tomogr* 2000;42:57–60
47. Casillas J, Joseph RC, Guerra JJ Jr. CT appearance of uterine leiomyomas. *Radiographics* 1990;10:999–1007
48. Sweet RI, Ledger WJ. Puerperal infectious morbidity: a two-year review. *Am J Obstet Gynecol* 1973;117:1093–1100
49. Langer JE, Dinsmore BJ. Computed tomographic evaluation of benign and inflammatory disorders of the female pelvis. *Radiol Clin North Am* 1992;30:831–842
50. Urban BA, Pankov BL, Fishman EK. Postpartum complications in the abdomen and pelvis: CT evaluation. *Crit Rev Diagn Imaging* 1999;40:1–21
51. Rooholamini SA, Au AH, Hansen GC, et al. Imaging of pregnancy-related complications. *Radiographics* 1993;13:753–770
52. Zuckerman J, Levine D, McNicholas MMJ, et al. Imaging of pelvic postpartum complications. *AJR* 1997;168:663–668
53. Wachsberg RH, Kurtz AB. Gas within the endometrial cavity at postpartum US: a normal finding after spontaneous vaginal delivery. *Radiology* 1992;183:431–433
54. Lydon-Rochelle M, Holt VL, Easterling TR, Martin DP. Risk of uterine rupture during labor among women with a prior cesarean delivery. *N Engl J Med* 2001;345:3–8
55. Twickler DM, Setiawan AT, Harrell RS, Brown CE. CT appearance of the pelvis after cesarean section. *AJR* 1991;156:523–526
56. Yassa NA, Ryst E. Ovarian vein thrombosis: a common incidental finding in patients who have undergone total abdominal hysterectomy and bilateral salpingo-oophorectomy with retroperitoneal lymph node dissection. *AJR* 1999;172:45–47
57. Jacoby WT, Cohan RH, Baker ME, et al. Ovarian vein thrombosis in oncology patients: CT detection and clinical significance. *AJR* 1990;155:291–294
58. Maldjian PD, Zurlow J. Ovarian vein thrombosis associated with a tubo-ovarian abscess. *Arch Gynecol Obstet* 1997;261:55–58
59. Brown CE, Stettler RW, Twickler D, Cunningham FG. Puerperal septic thrombophlebitis: Incidence and response to heparin therapy. *Am J Obstet Gynecol* 1999;181:143–148
60. Twickler DM, Setiawan AT, Evans RS, et al. Imaging of puerperal septic thrombophlebitis: prospective comparison of MR imaging, CT and sonography. *AJR* 1997;169:1039–1043
61. Van Hoe L, Baert AL, Marchal G, et al. Thrombosed ovarian vein collateral mimicking acute appendicitis on CT. *J Comput Assist Tomogr* 1994;18:643–646
62. Weinstein L. Syndrome of elevated liver enzymes, hemolysis, and low platelet count: a severe consequence of hypertension in pregnancy. *Am J Obstet Gynecol* 1982;142:159–167
63. McKenna J, Dover NL, Brame RG. Preeclampsia associated with hemolysis, elevated liver enzymes and low platelets: an obstetric emergency? *Obstet Gynecol* 1983;62:751–754
64. Killam AP, Dillard SH, Patton RC, Pederson PR. Pregnancy-induced hypertension complicated by acute liver disease and disseminated intravascular coagulation. *Am J Obstet Gynecol* 1975;123:823
65. Minakami H, Sugimoto H, Manaka C, et al. HELLP syndrome: CT evaluation. *Gynecol Obstet Invest* 1994;38:28–30